Molecular Neurobiology (2019) 56:502–512
https://doi.org/10.1007/s12035-018-1087-8

JM-20 Treatment After MCAO Reduced Astrocyte Reactivity and Neuronal Death on Peri-infarct Regions of the Rat Brain

Jeney Ramírez-Sánchez[1] · Elisa Nicoloso Simões Pires[2] · André Meneghetti[2] · Gisele Hansel[2] · Yanier Nuñez-Figueredo[1] · Gilberto L. Pardo-Andreu[3] · Estael Ochoa-Rodríguez[4] · Yamila Verdecia-Reyes[4] · René Delgado-Hernández[1] · Christianne Salbego[2,5] · Diogo O Souza[2,5]

Received: 5 December 2017 / Accepted: 12 April 2018 / Published online: 3 May 2018

Abstract

Stroke is frequently associated with severe neurological decline and mortality, and its incidence is expected to increase due to aging population. The only available pharmacological treatment for cerebral ischemia is thrombolysis, with narrow therapeutic windows. Efforts aimed to identify new therapeutics are crucial. In this study, we look into plausible molecular and cellular targets for JM-20, a new hybrid molecule, against ischemic stroke in vivo. Male Wistar rats were subjected to 90 min middle cerebral artery occlusion (MCAO) following 23 h of reperfusion. Animals treated with 8 mg/kg JM-20 (p.o., 1 h after reperfusion) showed minimal neurological impairment and lower GABA and IL-1β levels in CSF when compared to damaged rats that received vehicle. Immunocontent of pro-survival, phosphorylated Akt protein decreased in the cortex after 24 h as result of the ischemic insult, accompanied by decreased number of $NeuN^+$ cells in the peri-infarct cortex, cornu ammonis 1 (CA1) and dentate gyrus (DG) areas. Widespread reactive astrogliosis in both cortex and hippocampus (CA1, CA3, and DG areas) was observed 24 h post-ischemia. JM-20 prevented the activated Akt reduction, neuronal death, and astrocytes reactivity throughout the brain. Overall, the results reinforce the pharmacological potential of JM-20 as neuroprotective agent and provide important evidences about its molecular and cellular targets in this model of cerebral ischemia.

Keywords JM-20 · Neuroprotection · Middle cerebral artery occlusion · Akt · Astrocytes

Introduction

Stroke is frequently associated with severe neurological impairment and mortality. Its incidence is expected to increase due to prolonged life expectancy. Ischemic stroke is a consequence of a reduced or complete interrupted cerebral blood flow, which rapidly affects neural cells via a complex interplay of processes like excitotoxicity, neuroinflammation, and apoptosis [1, 2]. Thus far and despite many years of research, the only available pharmacological treatment for the acute phase of cerebral ischemia is the intravenous tissue plasminogen activator (tPA), yet within 4.5 h [3]. Thus, all efforts aimed to the identification of new therapeutic approaches directed to improve the recovery and quality of life of stroke patients are crucial.

A recent approach for the rational design of new candidates against ischemic stroke has gained worldwide attention: multitarget-directed molecules that include a variety of hybrid compounds acting simultaneously on diverse biological targets [4, 5]. Our group has developed a new multifunctional molecule, JM-20 (3-ethoxycarbonyl-2-methyl-4-(2-

✉ Diogo O Souza
00001192@ufrgs.br; diogo@ufrgs.br

1 Centro de Investigación y Desarrollo de Medicamentos, Ave 26, No. 1605 Boyeros y Puentes Grandes, CP 10600 Havana, Cuba

2 Programa de Pós-graduação em Bioquímica, Departamento de Bioquímica, ICBS, Universidade Federal do Rio Grande do Sul, Rua Ramiro Barcelos, 2600-Anexo I, Porto Alegre, Rio Grande do Sul 90035-003, Brazil

3 Centro de Estudio para las Investigaciones y Evaluaciones Biológicas, Instituto de Farmacia y Alimentos, Universidad de La Habana, ave. 23 # 21425 e/214 y 222, La Coronela, La Lisa, CP 13600 Havana, Cuba

4 Laboratorio de Síntesis Orgánica de La Facultad de Química, Universidad de La Habana, Zapata s/n entre G y Carlitos Aguirre, Vedado Plaza de la Revolución, CP 10400 Havana, Cuba

5 Departamento de Bioquímica, PPG em Bioquímica, PPG em Educação em Ciência, Instituto de Ciências Básicas da Saúde, Universidade Federal do Rio Grande do Sul, Rua Ramiro Barcelos, 2600 anexo, Porto Alegre, Rio Grande do Sul 90035-003, Brazil

nitrophenyl)-4,11-dihydro-1H-pyrido[2,3-b][1,5]benzodiazepine) [6], with promising neuroprotective effect against cerebral ischemia [7–12].

This 1,5-benzodiazepine fused to a dihydropyridine moiety has shown to possess several pharmacological effects in both, in vivo and in vitro models of brain ischemia [7, 9, 10]. Oral administration of JM-20 protects against permanent [11] and transient focal cerebral ischemia [9] in rats, involving anti-excitotoxic and mitoprotective mechanisms. A modulatory effect over glutamatergic system was also observed in synaptic vesicles, in which JM-20 reduced the H^+-ATPase activity and the vesicular glutamate uptake, whereas in cultured astrocytes and co-cultured neurons and astrocytes, the molecule increases the neurotransmitter uptake [8]. A first approach to the anti-inflammatory and anti-apoptotic properties of JM-20 was conducted in organotypic hippocampal slice cultures deprived of oxygen and glucose (OGD) to resemble ischemia/reperfusion damage [7].

Now, our group aimed to evaluate the effects of middle cerebral artery occlusion (MCAO) and JM-20 on astrocytes reactivity in peri-infarct regions of the rat brain and on the release of pro- and anti-inflammatory cytokines (IL-1β and IL-10, respectively). Taking into account that PI3K/Akt cell signaling pathway may have a role in preventing cellular death after JM-20 treatment, as was previously demonstrated [7], here, we assessed Akt activation and neuronal survival after MCAO. Finally, the concentration of gamma-aminobutyric acid (GABA) in the cerebrospinal fluid (CSF) was also investigated in order to evaluate if the effect of JM-20 may involve the release of this inhibitory neurotransmitter.

Materials and Methods

Animals

Adult male Wistar rats (CENPALAB, Havana, Cuba) weighing 260–285 g were housed under controlled light and environmental conditions (12 h light/dark cycle at a temperature of 22–24 °C) with water and commercial food ad libitum. All experimental procedures were performed in accordance with national and institutional guidelines under approved animal protocols (Animal Care Committee of Federal University of Rio Grande do Sul, Brazil and CIDEM, Havana, Cuba). All efforts were made to prevent suffering and to minimize the number of animals used.

MCAO-Induced Focal Cerebral Ischemia

MCAO and reperfusion were performed as previously described, using an intraluminal filament model [13]. Briefly, anesthesia was induced with ketamine (75 mg/kg, i.p.) and xylazine (8 mg/kg, i.p.). The right carotid region was exposed, and the external and common carotid arteries were ligated with a 3-0 silk suture. A 25 mm length 4-0 nylon monofilament (Somerville, Brazil), whose tip had been rounded and coated with poly-L-lysine [14, 15], was introduced (18–20 mm) through the internal carotid artery, thereby occluding the MCA origin. After 90 min of MCAO, reperfusion was permitted by gentle withdrawal of the suture (under the same anesthetic conditions as surgery). Until recovery, body temperature was maintained within the normal range (from 36.5 to 37.5 °C) using a heating pad. Control animals undergo sham surgery without suture insertion. Twenty-three hours after reperfusion, functional outcomes were evaluated, animals were sacrificed, and brains were rapidly removed for further analysis.

Drug Treatment and Experimental Groups

The behavior of the rats subjected to MCAO was examined after recovery from surgery, and only those animals showing contralateral forelimb dysfunction were included for further experimentation. Animals were randomly assigned to four groups: (1) control ischemia/reperfusion (I/R) group treated with vehicle, (2) I/R treated with 8 mg/kg JM-20, sham-operated group treated with vehicle, and (4) sham-operated group treated with 8 mg/kg JM-20. JM-20 was synthesized, purified, and characterized as previously reported [6]. A single dose of the drug or vehicle was orally administered (by gastric gavage) 1 h after reperfusion (2½ hours after ischemia onset) ensuring a constant volume of 4 mL/kg. JM-20 was suspended in a 0.05% (*w*/*v*) carboxymethylcellulose (CMC) solution (vehicle) immediately before use. The dose of JM-20 was selected based on our previous results [9].

Neurological Deficit Scoring

Neurobehavioral deficits were assessed according to a six-point scale: 0 = no observable neurological deficits, 1 = failure to extend left forepaw fully, 2 = circling to the left if pulled by tail, 3 = spontaneously circling to the left, 4 = no spontaneous activity with a depressed level of consciousness, and 5 = death [14, 16].

CSF and Tissue Processing

After 23 h of reperfusion, rats were anesthetized, placed in a stereotaxic apparatus, and CSF samples (about 60 μL per rat) were drawn by direct puncture of the cisterna magna with an insulin syringe (27-gauge ½ inch needle) [17, 18]. In order to obtain cell-free supernatants, all samples were centrifuged at 10,000×*g* in an Eppendorf centrifuge during 5 min and stored (− 80 °C) until analysis.

For P-Akt/Akt expression analysis by western blotting, dorsal segments of three cortical regions (~ 2 mm thick) were

dissected out from ipsilateral hemisphere to be separately analyzed: + 4.20 to + 2.20, + 1.20 to − 0.80, and − 1.70 to − 3.70 mm A.P. with respect to Bregma (Fig. 1) [19]. In the case of glial fibrillary acidic protein (GFAP) expression, analysis was conducted in a single slice (approximately + 4.20 to − 3.70 mm A.P. with respect to Bregma). The tissue was homogenized using lysis solution [4% sodium dodecylsulfate (SDS), 2.1 mM EDTA, and 50 mM Tris-HCl, pH 6.8] containing a protease (p8340, Sigma, St. Louis, MO, USA) and phosphatase inhibitors cocktail (sc-45045, Santa Cruz, CA, USA). Aliquots were taken for protein determination [20] and the homogenates were normalized with sample buffer [62.5 mM Tris-HCl, pH 6.8, 2% (*w*/*v*) SDS, 5% b-mercaptoethanol, 10% (*v*/*v*) glycerol, 0.002% (*w*/*v*) bromophenol blue].

For immunohistochemical analysis, the animals were transcardially perfused with 0.9% saline followed by 4% paraformaldehyde in 0.1 M phosphate buffer (pH 7.4). The brains were removed and post-fixed in the same solution at room temperature overnight and then were incubated in a 30% sucrose solution for 2 days. Coronal slices (50 μm) were obtained using a Vibratome (Leica Biosystems, Mannheim, Wetzlar, Germany). Three slices taken through the rostrocaudal axis from prefrontal and frontoparietal cortex and hippocampus (nine slices total) were selected per animal. In the cortex, analyses were conducted in the peri-infarct area of the ischemic brains or anatomically similar area in sham animals (Fig. 1). In the hippocampus, the cornu ammonis 1 (CA1), CA3, and dentate gyrus (DG) subregions were identified, according to Paxinos and Watson [19].

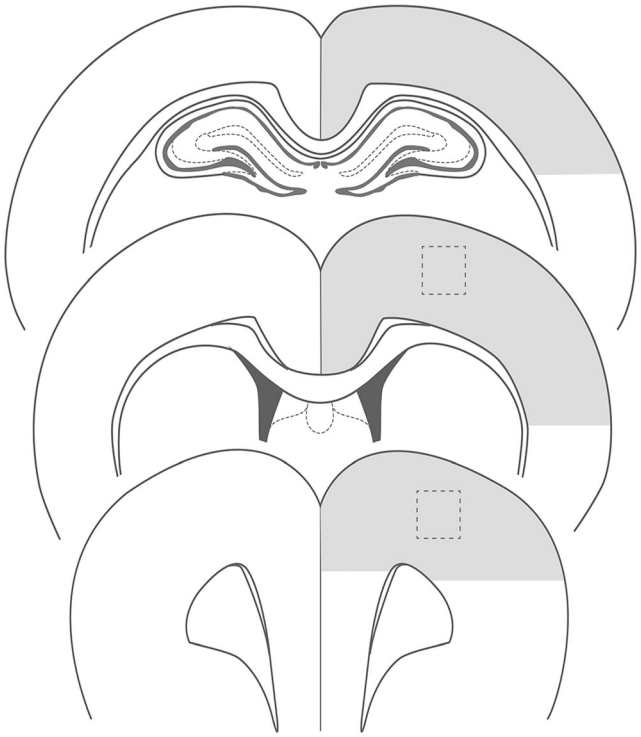

Fig. 1 Schematic illustration showing cortical regions analyzed by Western blot (gray). Immunohistochemistry (dotted square) was conducted in peri-infarct regions of the cortex and also in hippocampus (CA1, CA3, and DG subregions)

Determination of Cytokine Levels in CSF

Pro-inflammatory interleukin-1β (IL-1β) and anti-inflammatory interleukin-10 (IL-10) cytokine concentrations in CSF were measured using specific enzyme-linked immunosorbent assay (ELISA) kits according to the recommendations of the supplier (R&D Systems). The results are expressed as picogram per milliliter (pg/mL).

HPLC Procedure

High-performance liquid chromatography (HPLC) was used to quantify the GABA levels in CSF cell-free supernatant aliquots [21]. Briefly, samples were filtered and derivatized with o-phthalaldehyde and mercaptoethanol. CSF samples were separated with a reverse phase column (Supelcosil LC-18, 250 mm × 4.6 mm, Supelco) in a Shimadzu Instruments liquid chromatograph. The mobile phase flowed at a rate of 1.4 mL/min, and column temperature was 24 °C. Buffer composition was A, 0.04 mol/L $NaH_2PO_4 \cdot H_2O$ buffer, pH 5.5, containing 20% of methanol; and B, 0.01 mol/L $NaH_2PO_4 \cdot H_2O$ buffer, pH 5.5, containing 80% of methanol. The gradient profile was modified according to the content of buffer B in the mobile phase: 0% at 0.00 min, 50% at 30 min, 100% at 30.01–35.00 min, and 0% at 35.01–40.00 min. Absorbance was read at 360 and 455 nm, excitation and emission, respectively, in a Shimadzu fluorescence detector. Concentration of GABA was expressed in micromolar [22].

Western Blot Analysis

To investigate the phosphorylation status of Akt, proteins (50 μg per lane) were resolved on 12% SDS-PAGE and transferred to nitrocellulose membranes using a semi-dry transfer apparatus (Bio-Rad Trans-Blot SD, Hercules, CA, USA). Membranes were incubated for 60 min at 4 °C in blocking solution (Tris-buffered saline containing 5% powdered skim milk and 0.1% Tween-20, pH 7.4) and further incubated overnight at 4 °C with the appropriate primary antibody dissolved in the blocking solution. The primary antibodies anti-phosphorylated Akt (Ser473; P-Akt, 1:1000, Cell Signaling Technology), anti-Akt (1:1000; Cell Signaling Technology), anti-GFAP (1:3000, Sigma), and anti-β-actin (1:1000, Cell Signaling Technology) were used. The membranes were then incubated with horseradish peroxidase-conjugated secondary antibody (1:2000, Amersham Pharmacia Biotech, Piscataway, NJ, USA) for 2 h. The chemiluminescence (ECL, Amersham Pharmacia Biotech) was detected using X-ray films (Kodak

X-Omat, Rochester, NY, USA) that were scanned, and bands were quantified using ImageJ 1.50 software (National Institutes of Health, USA). Data are expressed as percentage of control values.

Immunohistochemistry

Sections from specified regions were permeabilized and blocked during 2 h with phosphate-buffered saline (PBS), pH 7.4, containing 3% BSA and 0.1% Triton X-100. Then, slices were incubated overnight at 4 °C with the following primary antibodies: mouse anti-neuron-specific nuclear protein (NeuN, 1:500, Sigma) and rabbit anti-GFAP (1:500, Sigma) to label astrocytes.

After rinsing in PBS, antigens were visualized with appropriate secondary antibodies: Alexa Fluor 594-conjugated goat anti-mouse (1:500, Invitrogen) or Alexa Fluor 488-conjugated donkey anti-rabbit (1:500, Invitrogen). Tissues were counterstained with DAPI (1:1000, 0.1%, Sigma) and mounted in DPX Mounting Medium (Sigma). All images were captured with an Olympus IX70 Microscope (Olympus, Tokyo, Japan) and further analyzed using ImageJ 1.50 software (National Institutes of Health, USA). Adobe Photoshop was used as a digital layout tool for composition and overlay of acquired images.

For quantitative analyses, $NeuN^+$ cells with intact and round nuclei were counted as surviving neurons. To evaluate morphological aspects of astrocytes, $GFAP^+$ cells with clearly visible cell nuclei and soma were selected and the length of the longest cellular processes (the distance between the nucleus and the tip of an extended process) was measured using the plugin NeuronJ of the ImageJ 1.50 software.

Statistical Analysis

GraphPad Prism 7.0 software (GraphPad Software Inc., USA) was used to determine significant differences among experimental groups. The data were expressed as the mean ± SEM. Comparisons among different groups were performed by unpaired *t* test (neurological score), one-way analysis of variance (ANOVA) followed by the Newman-Keuls multiple comparison test, or two-way ANOVA followed by the Dunnett's multiple comparison test (NeuN-positive cells). Correlation was analyzed by Pearson's correlation. Differences were considered statistically significant at $P < 0.05$.

Results

JM-20 Improved Functional Outcome After Transient MCAO

The behavioral examination was carried out 24 h after the MCAO surgery to investigate whether JM-20 effects promoted neurological recovery. In contrast with sham-operated animals (vehicle- or JM-20 treated, data not shown), ischemic rats showed a clear contralateral motor deficit (Fig. 2) accordingly to the neurological scale used. The most frequently observed clinical sign of cerebral damage was the spontaneously circling to the left likely due to the paralysis of the contralateral forelimb. In contrast, treatment with JM-20 significantly reduced ($P < 0.05$) the behavioral deficit caused by the ischemia so that decreasing the neurological score related to movement and posture abnormalities. The results confirm previous work [9] showing that acute, oral treatment with the drug consistently improves functional outcomes after ischemic stroke in rats.

Effects of JM-20 on IL-1β, IL-10, and GABA Levels in CSF of Ischemic Rats

The detection of biological markers in CSF, including neurotransmitters and inflammatory mediators, has proven to be useful for diagnosis, and pathological and pharmacological studies of different neurological diseases in humans and rodents [18, 23]. Here, we investigated the effect of JM-20 on GABA, pro-inflammatory (IL-1β), and anti-inflammatory (IL-10) cytokine levels in CSF as indicative of an unbalance in neurotransmitter release and inflammatory response, respectively. Transient MCAO augmented the concentration of GABA in comparison with sham treated with vehicle and sham treated with JM-20 groups (4.56 ± 0.68 vs 3.07 ± 0.73 and 3.25 ± 0.74; $P < 0.05$) (Fig. 3a). The treatment with JM-20 did not modify the levels of GABA when comparing (3.69 ± 0.61; $P > 0.05$) versus either sham or ischemic rats.

A correlation analysis between the levels of excitatory amino acids (EAA) in the CSF (previously published by our group) [9] and the GABA concentrations showed here was performed. Animals with elevated glutamate and aspartate levels also showed higher GABA concentrations (i.e., ischemic group), indicating that the increment of this inhibitory neurotransmitter may be related to the EAA increase after MCAO. The analysis revealed that there was a moderate positive correlation ($r = 0.52$, $P = 0.03$; Fig. 3b) between GABA and glutamate concentrations and a strong positive correlation between GABA and aspartate concentrations ($r = 0.62$, $P = 0.008$; Fig. 3b).

Figure 4a, b shows that MCAO surgery did not alter the levels of cytokines (pg/mL) (IL-1β and IL-10; 291.8 ± 28 and 152.9 ± 24, respectively) in the CSF since differences with respect to sham treated with vehicle (240.9 ± 10 and 180.3 ± 5) were not detected ($P > 0.05$). Although JM-20 produced no effects in IL-10 release (172.4 ± 14) when comparing with all groups, it produced a significant ($P < 0.05$) decrease of IL-1β (180.9 ± 24) with respect to vehicle-treated ischemic rats. Differences in this pro-inflammatory cytokine levels between

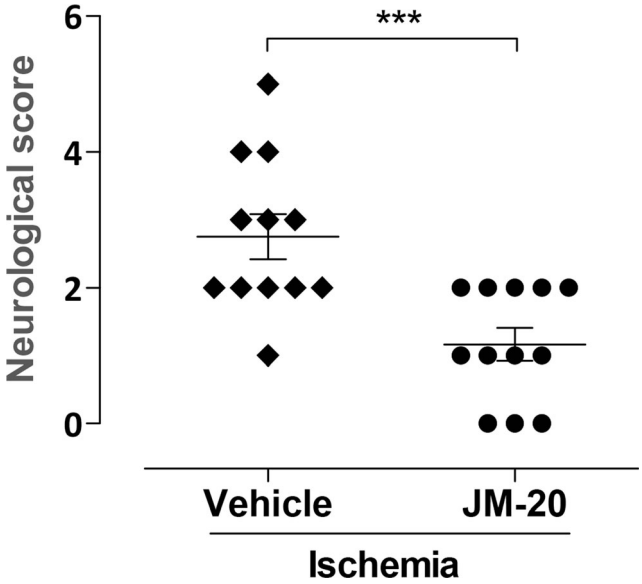

Fig. 2 Post-ischemic JM-20 treatment improved the functional outcome after experimental stroke. No neurological impairment was observed in sham-operated animals (results not shown), but severe deficit was detected in the vehicle-treated MCAO group, related to circling movements, paw flexion, and decreased spontaneous movements. JM-20 treatment (8 mg/kg, single dose) 1 h after reperfusion significantly reduced the neurological score, improving functional performance of the ischemic rats. ***$P < 0.001$ by unpaired t test, $n = 12$ per group. Data represent individual scores and mean ± S.E.M are also plotted

ischemia and sham treated with JM-20 group (160.5 ± 26, $P < 0.05$) were also observed.

JM-20 Prevented the Decrease of P-Akt and the Increase of GFAP Expression Induced by Ischemia in the Cerebral Cortex

To look into possible mechanisms by which JM-20 exerts the neuroprotective effects observed here, we explored the PI3K cell signaling pathway by measuring the phosphorylation state of the protein kinase Akt, through western blotting. Several regions of the cerebral cortex were studied (as represented in Fig. 1).

Pro-survival, P-Akt diminished after MCAO at the end of the reperfusion period in all cortical regions, as shown in Fig. 5a, b. The P-Akt/Akt ratio falls by approximately 0.5 times in prefrontal (+ 4.20 to + 2.20 mm) and frontoparietal cortices (+ 1.20 to − 0.80 and − 1.70 to − 3.70 mm A.P. with respect to Bregma) when compared to sham values ($P < 0.05$). The levels of P-Akt in ischemic rats treated with JM-20 were similar to those in sham-operated animals ($P > 0.05$) but significantly higher when compared to vehicle-treated ischemic rats [$P < 0.001$ in the prefrontal cortex, $P < 0.01$ and $P < 0.05$ in frontoparietal cortex (+ 1.20 to − 0.80 and − 1.70 to − 3.70 mm, respectively)]. Figure 5a, b also reflects that no difference ($P > 0.05$) in total Akt was observed.

Regarding GFAP immunocontent in cortex, we observed (Fig. 5d) that JM-20 counteracted the ischemia-induced increase of this astrocytic marker. GFAP immunocontent (% of control) is almost 45% higher than sham (either vehicle- or JM-20 treated, $P < 0.05$) and ischemic rats that received drug treatment ($P < 0.05$).

Reactive Astrogliosis Accompanied Neuronal Death in Peri-infarct Cortex, CA1, and DG and Extended to CA3: Effects of JM-20

The effect of I/R on neuronal survival and astrocyte reactivity was investigated in several regions of the rat brain using NeuN and GFAP immunostaining, respectively (Fig. 6). Results in Table 1 evidenced that ischemic damage in animals receiving vehicle treatment extended to peri-infarct regions of the prefrontal (44 ± 5 $NeuN^+$ cells/0.1 mm^2) and frontoparietal (56 ± 11 $NeuN^+$ cells/0.1 mm^2) cortices and to CA1 (107 ± 17 $NeuN^+$ cells/0.1 mm^2) and DG (199 ± 21 $NeuN^+$

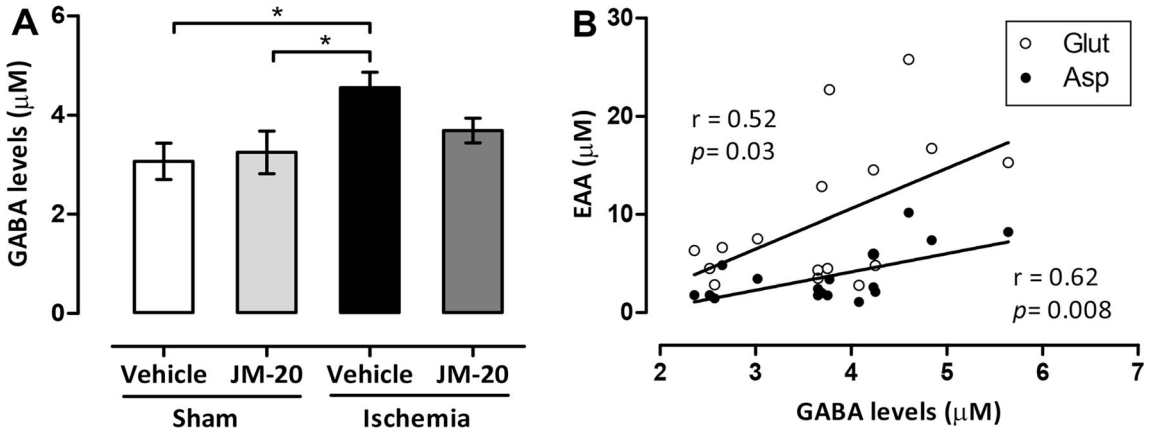

Fig. 3 Effect of JM-20 treatment on GABA levels in CSF of ischemic rats. Cerebrospinal fluid was collected 23 h after reperfusion and analyzed by HPLC to determine GABA concentration (**a**). Correlation between excitatory amino acids (EAA) and GABA concentrations is also depicted (**b**). Bars represent mean values ± SEM ($n = 4$–6 per group). *$P < 0.05$ by ANOVA and post hoc Newman-Keuls Multiple Comparison tests

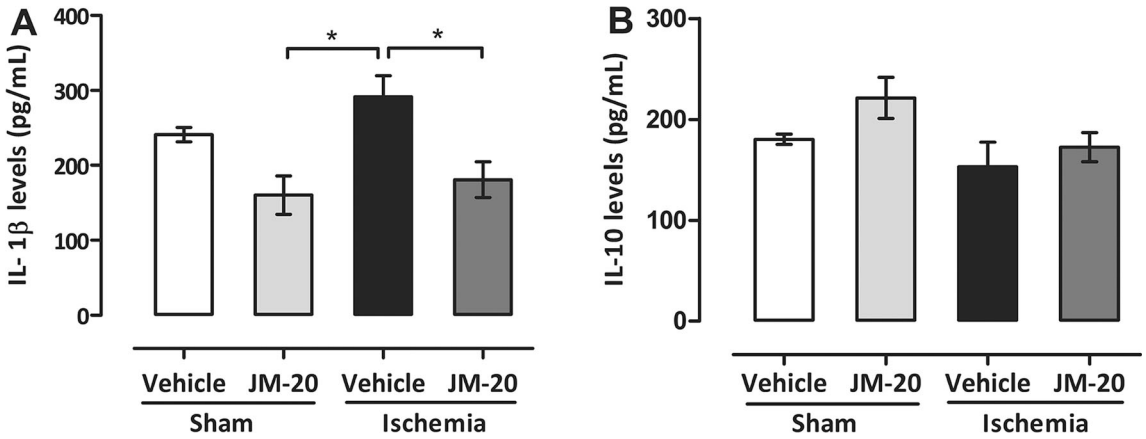

Fig. 4 Effect of JM-20 treatment on IL-1β (**a**) and IL-10 (**b**) concentrations in CSF of ischemic rats. Cerebrospinal fluid was collected 23 h after reperfusion and analyzed by HPLC. Bars represent mean values ± SEM ($n = 4$–6 per group). *$P < 0.05$ by ANOVA and post hoc Newman-Keuls Multiple Comparison tests

cells/0.1 mm^2) subregions of hippocampus, all showing decreased number of NeuN$^+$ cells and abundant cells with vacuolated nucleus (respect to sham-vehicle group). GFAP immunoreactive cells augmented not only in these regions with respect to sham groups but also in CA3. Treatment with JM-20 prevented both the decrease of NeuN$^+$ cells (prefrontal cortex and CA1) and the increase of GFAP$^+$ cells in all studied regions except CA3, comparing with control ischemic rats, and showed no statistically significant differences ($P > 0.05$) when compared with sham-vehicle group.

The degree of hypertrophy of astrocytes was assessed by measuring the longest processes of GFAP$^+$ cells from specified regions. The length of primary astrocytic processes was similar in sham animals receiving vehicle or JM-20, as shown in Table 1. On MCAO-lesioned rats, however, astrocytes exhibited prominent signs of hypertrophy since GFAP$^+$ processes were longer than in the sham groups (Fig. 6) on all prefrontal and frontoparietal cortices and hippocampus (CA1, CA3, and DG). Enlargement of the astrocytic processes 24 h post-MCAO was effectively inhibited by JM-20 treatment.

Together, these findings indicate that 90 min MCAO and further reperfusion affect neuronal viability and astrocyte function even in distal, peripheral regions of the lesion, and JM-20 treatment is able to inhibit it, thus providing neuroprotection.

Discussion

Population aging has been growing a lot in recent decades, and the twenty-first century will witness even more rapid aging than did the century just past. Therefore, despite the advances in public health and medicine, the age-related disease (including stroke) incidence has not changed [24].

Cerebral ischemia, the most prevalent form of stroke, occurs when a thrombus or an embolus blocks the blood flow to parts of the brain [2]. Stroke patients often have to confront a neurological decline that limits physical, psychological, and functional aspects of living. Recently, the design of drugs able to interact with different targets involved in the pathological cascade of neurodegenerative diseases has emerged as alternative to reach (or to improve) therapeutic effectiveness. These multi-target-directed ligands contain different pharmacophore moieties from identified bioactive molecules, and its development allows the simplification of therapeutic regimen and obviates the challenge of simultaneously administering multiple drugs [25].

JM-20 was first identified as a suitable candidate for use in cerebral ischemia few years ago [10]. This multipotent molecule was specifically developed to combine the GABAergic activity of benzodiazepines with anti-calcic effects of dihydropyridines.

In the present study, we evaluated the neuroprotective effect of JM-20 treatment on neurological status, as well as on some neurochemical parameters, in rats subjected to transient cerebral ischemia (90 min MCAO). With respect to functional benefits (Fig. 2), our results are in accordance with previous studies demonstrating that JM-20 protected rats from neurological impairment and death [9, 11].

In our previous report about the neuroprotective mechanisms of JM-20, we showed that the concentration of EAA (glutamate and aspartate) increased in the CSF of MCAO-induced ischemic rats [9]. Now, we focused on GABA, and we observed that it is also increased, as seen in Fig. 3a, which indicates that the ischemic insult impaired both excitatory and inhibitory neurotransmission. Based on the correlation that we found between both effects (showed in Fig. 3b), the higher concentration of GABA in the CSF after MCAO may reflect an increase in the release of GABA as a self-defense mechanism in an attempt to counteract excitotoxicity, like what has been previously suggested on the literature [26, 27].

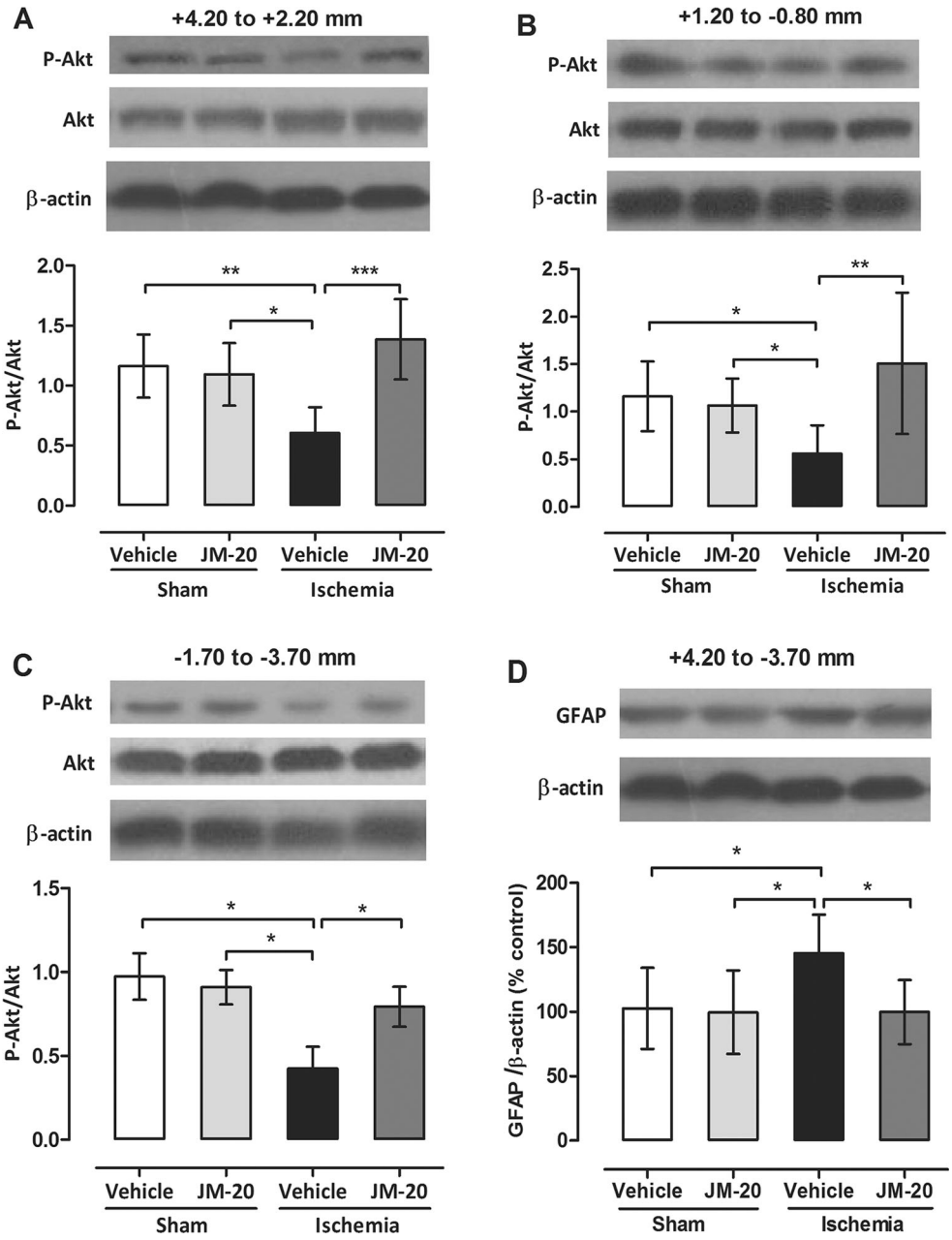

Fig. 5 Western blot analysis of Akt and GFAP expression in the rat cortex 24 h post-MCAO. **a–c** Representative blotting and quantitative analyses of the phosphorylation state of Akt (expressed as pAkt/Akt ratio) in three cortical regions distributed throughout the anteroposterior axis of the frontoparietal cortex. **d** Representative blotting and quantitative analyses of the immunocontent of GFAP. Proteins were normalized by β-actin and presented as a percent of control (sham-operated animals, 100%). Data are mean ± S.E.M ($n = 5–8$ per group). $^{*}P < 0.05$, $^{**}P < 0.01$, $^{***}P < 0.001$, by ANOVA and post hoc Newman–Keuls Multiple Comparison tests

On the other hand, the treatment with JM-20 prevented the increase of GABA, likely due to a secondary effect of the drug against excitotoxicity and neuronal death, since the treatment diminished EAA levels and infarct as well [9].

The levels of cytokines appear altered in CSF and serum after cerebral ischemia in rodents and humans [28, 29]. However, we did not observe a significant effect induced by 23 h of I/R on pro-inflammatory IL-1β and anti-inflammatory IL-10 (when compared with sham-vehicle group). The result is in part contradictory because cytokines are usually used as biochemical markers of inflammation caused by stroke. Although several techniques have been described for the collection of CSF from rats, unfortunately, blood contamination arises like a common problem for these techniques [30, 31]. Taken these facts into account, and also that JM-20 decreased the IL-1β when compared to ischemia-vehicle group, as we can see in Fig. 4a, we suggest further studies in which the levels of cytokines would be measured in the cerebral tissue, allowing the selection of specified regions of interest (e.g., ischemic penumbra) and to avoid the contamination with blood. Immunohistochemical studies for activated microglia should be also included, since neuroinflammatory response is mainly attributed to glial cells (i.e., astrocytes and microglia).

Stroke lesions are considered to involve focal and peri-focal zones. In the rat, the focal area (the "ischemic core") after MCAO usually comprise the lateral part of the

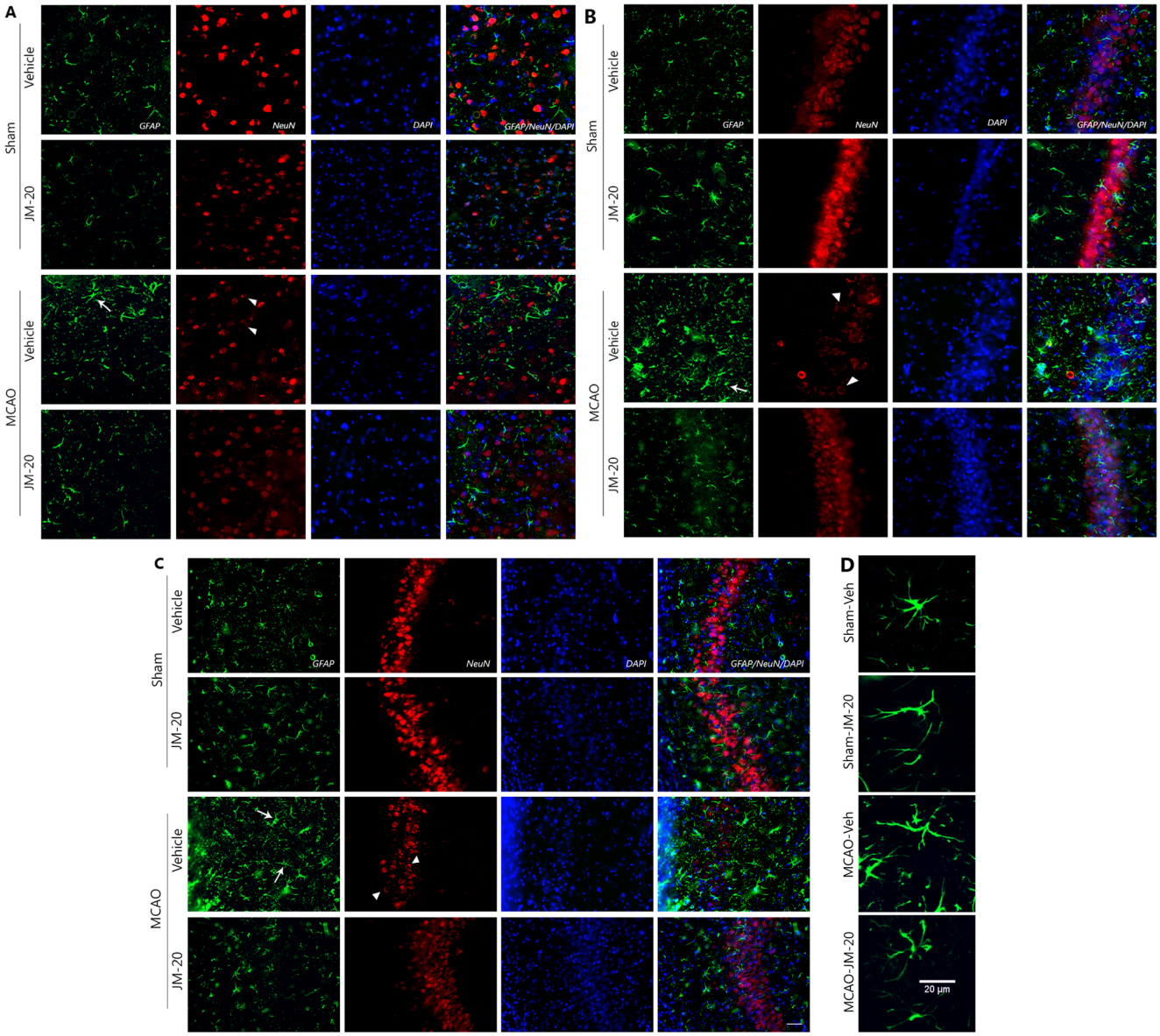

Fig. 6 Representative photomicrographs of peri-infarct regions of the rat brain after ischemia/reperfusion. Rats received 8 mg/kg JM-20 or vehicle (p.o.; sham and MCAO-injured rats) 1 h post-reperfusion. Coronal sections from prefrontal and parietal cortex (**a**) and from hippocampal subregions CA1 (**b**), CA3 (**c**), and DG were immunostained using neuron-specific nuclear protein (NeuN) and the astrocytic marker glial fibrillary acidic protein (GFAP). Arrowheads show neurons with diminished reactivity and vacuolated nuclei. Illustrative $GFAP^+$ astrocytes with enlarged processes are indicated with arrows. **d** Enlargement of representative astrocytic cells from CA3. The treatment with JM-20 increased the number of surviving neurons reducing the number of hypertrophic astrocytes as well. Scale bar = 40 (**a**, **b**, **c**) or 20 μm (**d**)

caudoputamen and the overlying neocortex, while the latter (the "penumbra") consists of large parts of the neocortex which are not sufficiently supplied by collateral flow [32, 33]. The ischemic penumbra has received considerable attention of researchers because neural cells can be potentially salvaged from death by recirculation and drug administration.

In this work, peri-infarct areas were chosen considering the literature and our own experience. Immunohistochemical analyses were directed to the adjacent zones to those critically damaged accordingly with TTC staining [9]. Our results confirmed that JM-20 actually limits the extension of the brain injury. Ischemia caused a reduction in the number of intact neurons (NeuN immunoreactivity, Table 1 and Fig. 6) in susceptible areas of the brain, that is, cortex and CA1 [34, 35]. The effect of JM-20 preventing neuronal death is likely related to its ability to prevent the decrease of P-Akt (Fig. 5), a protein kinase involved in pro-survival pathways [36–38]. The assumption is additionally supported by previous studies in which this effect accompanied the reduction of direct (GSK-3β) and indirect (caspase-3) pro-apoptotic downstream targets

Table 1 Immunohistochemical analysis by brain regions 24 h post-ischemia

	Sham-vehicle	Sham-JM-20	MCAO-vehicle	MCAO-JM-20
$NeuN^+$ cells/0.1 mm^2				
Prefrontal cortex	90 ± 7*	107 ± 4*	44 ± 5	73 ± 4
Parietal cortex	105 ± 5*	141 ± 7***	56 ± 11	107 ± 7*
CA1	171 ± 6**	178 ± 10**	107 ± 17	201 ± 13***
CA3	128 ± 12	132 ± 9	112 ± 12	135 ± 10
DG	267 ± 20**	202 ± 21	199 ± 21	203 ± 23
$GFAP^+$ cells/0.1 mm^2				
Prefrontal cortex	29 ± 4*	24 ± 6**	39 ± 8	30 ± 6*
Parietal cortex	30 ± 6**	29 ± 6**	42 ± 4	31 ± 6**
CA1	35 ± 8***	41 ± 9**	69 ± 21	45 ± 13**
CA3	39 ± 11*	41 ± 11*	57 ± 16	49 ± 10
DG	55 ± 10**	56 ± 14*	76 ± 13	53 ± 14**
Length of the longest astrocytic processes (GFAP) (μm)				
Prefrontal cortex	21.4 ± 2.7*	21.5 ± 4.8*	25.3 ± 3.9	20.8 ± 5.0**
Parietal cortex	19.9 ± 2.7**	20.9 ± 2.9**	24.0 ± 2.9	20.6 ± 3.6**
CA1	22.3 ± 2.5*	22.2 ± 4.4**	25.6 ± 2.8	21.7 ± 4.7**
CA3	21.4 ± 4.3*	21.5 ± 3.0*	24.4 ± 3.7	21.0 ± 3.4*
DG	18.3 ± 4.7**	21.4 ± 3.7*	23.6 ± 3.9	19.9 ± 4.6*

Data are shown as mean ± SEM

*$P < 0.05$, **$P < 0.01$, ***$P < 0.001$ versus MCAO-vehicle

of P-Akt in organotypic hippocampal cultures subjected to OGD and treated with JM-20 [7].

Today, many essential functions for astrocytes in healthy CNS had been recognized. They are involved in the metabolic and ionic homeostasis, establishment and maintenance of the blood brain barrier, trophic support of neurons, and also in the control of several aspects of the synaptic transmission [39, 40]. Under pathological situations, however, the role of astrocytes is less clear and remains controversial due to the molecular complexity of the reactive astrogliosis. The latter constitutes a response of astrocytes seen in pathological situations such as ischemia. Reactive astrocytes exhibit altered expression of many genes and distinct functional and morphological features, often including proliferation [41–43]. Controlled activation of astrocytes is considered beneficial to neurons, but reactive astrocytes may lose their neuroprotective functions or even gain neurotoxic properties.

Here, immunohistochemical analysis for GFAP showed that astrogliosis resulted from transient ischemia in rats treated with vehicle in those regions where neuronal survival was affected and even in those where not, such as CA3. Since reactive astrocytes were observed under both situations, to determine whether astrocytes negatively or positively contribute to neuronal fate results is difficult to explain.

The observed differences between hippocampal subregions with respect to the cellular response that ultimately lead to selective vulnerability/resistance to injury remain incompletely understood but could be related to astrocytes response [44, 45]. As discussed by Anderson et al., reactive astrocytes exhibit a large potential for heterogeneity at multiple levels, including gene expression, topography (distance from lesions), CNS regions, local (among neighboring cells), cell signaling, and function [40]. In summary, beyond the discussed effects that ischemia could exert directly on astrocytes, we should not overlook that astroglia may be responding to changes in their environment such as alterations in extracellular ions and amino acids, and to transient postischemic changes in neurons, even in those regions less susceptible to ischemia [35].

Our results suggest that astrocytes could constitute a cellular target for JM-20 treatment. Here, we demonstrated that GFAP immunopositive cells and morphological changes, assessed as length of the longest astrocytic process, became reduced following treatment in all regions. Previously, we showed that JM-20 (10 μM) increased GFAP immunoreactivity in CA1 and DG in organotypic hippocampal cultures exposed to OGD [7], when compared with vehicle-treated cultures. Apparently contradictory with the effect described here, differences between both studies could be ascribed to the type of injury (60 min OGD vs 90 min MCAO) and how neural cells respond to that injury. While OGD did not modify GFAP reactivity and therefore did not cause astrogliosis, MCAO actually induced astrocyte response after 23 h of reperfusion. On the other hand, neuroprotective role of JM-20 (limiting neuronal death) was seen associated to GFAP increase in the former and to reducing astrocyte reactivity in the later, both counteracting deleterious consequences of damage inductors.

In the author's opinions, certain interesting issue originates from the exposed results. First, as we discussed earlier, neuroinflammation after MCAO and further reperfusion were indirectly measured through the levels of cytokines in CSF, but microglia activation, a main player in the inflammatory response, remains unexamined. Second, we have demonstrated an inhibitory effect of JM-20 over reactive astrogliosis at early post-reperfusion period after the ischemic insult, but long-term impacts on post-ischemic recovery and astrocytes functionality of these effects should be addressed in the future.

In conclusion, we confirmed that JM-20 treatment reduced clinical signs of neurological deterioration induced by 90 min of MCAO. Ischemic animals treated with this multifunctional molecule showed concentrations of GABA and IL-1β in CSF that were similar to those observed in sham-operated animals. On the other hand, the reduction of neuronal death in the ipsilateral hemisphere afforded by JM-20 after MCAO was associated with (1) the activation of the pro-survival protein Akt and (2) the inhibition of widespread reactive astrogliosis in the peri-infarct regions of the rat brain, indicating some molecular and cellular target for JM-20 therapy in experimental stroke. Recently, the development of strategies to protect normal astrocyte physiology and function has emerged as a new alternative to improved therapeutic efficacy of novel neuroprotectants, and thus, the results provide new experimental evidences about JM-20 potential to promote post-stroke recovery.

Acknowledgements This work was supported by Coordenação de Aperfeiçoamento de Pessoal de Nível Superior (CAPES)-Brazil/Ministerio de Educación Superior (MES)-Cuba projects 140/11 and 092/10, Instituto Nacional de Ciência e Tecnologia para Excitotoxicidade e Neuroproteção (INCTEN)/Conselho Nacional de Desenvolvimento Científico e Tecnológico (CNPq), IBN.Net/CNPq, Fundação de Amparo à Pesquisa do Estado do Rio Grande do Sul (FAPERGS), and the Non-Governmental Organization MEDICUBA-SPAIN. We would like to thank to Dr. Nancy Pavón Fuentes for the scientific advising.

Compliance with Ethical Standards

Conflict of Interest The authors declare no conflict of interest.

References

1. Dirnagl U, Iadecola C, Moskowitz MA (1999) Pathobiology of ischaemic stroke: an integrated view. Trends Neurosci 22:391–397
2. Doyle KP, Simon RP, Stenzel-Poore MP (2008) Mechanisms of ischemic brain damage. Neuropharmacology 55(3):310–318. https://doi.org/10.1016/j.neuropharm.2008.01.005
3. George PM, Steinberg GK (2015) Novel stroke therapeutics: unraveling stroke pathophysiology and its impact on clinical treatments. Neuron 87(2):297–309. https://doi.org/10.1016/j.neuron.2015.05.041
4. Zhang Z, Zhang G, Sun Y, Szeto SS, Law HC, Quan Q, Li G, Yu P et al (2016) Tetramethylpyrazine nitrone, a multifunctional neuroprotective agent for ischemic stroke therapy. Sci Rep 6:37148. https://doi.org/10.1038/srep37148
5. Lorrio S, Gomez-Rangel V, Negredo P, Egea J, Leon R, Romero A, Dal-Cim T, Villarroya M et al (2013) Novel multitarget ligand ITH33/IQM9.21 provides neuroprotection in in vitro and in vivo models related to brain ischemia. Neuropharmacology 67:403–411. https://doi.org/10.1016/j.neuropharm.2012.12.001
6. Figueredo YN, Rodriguez EO, Reyes YV, Dominguez CC, Parra AL, Sanchez JR, Hernandez RD, Verdecia MP et al (2013) Characterization of the anxiolytic and sedative profile of JM-20: a novel benzodiazepine-dihydropyridine hybrid molecule. Neurol Res 35(8):804–812. https://doi.org/10.1179/1743132813Y.0000000216
7. Ramirez-Sanchez J, Simoes Pires EN, Nunez-Figueredo Y, Pardo-Andreu GL, Fonseca-Fonseca LA, Ruiz-Reyes A, Ochoa-Rodriguez E, Verdecia-Reyes Y et al (2015) Neuroprotection by JM-20 against oxygen-glucose deprivation in rat hippocampal slices: involvement of the Akt/GSK-3beta pathway. Neurochem Int 90:215–223. https://doi.org/10.1016/j.neuint.2015.09.003
8. Nunez-Figueredo Y, Pardo Andreu GL, Oliveira Loureiro S, Ganzella M, Ramirez-Sanchez J, Ochoa-Rodriguez E, Verdecia-Reyes Y, Delgado-Hernandez R et al (2015) The effects of JM-20 on the glutamatergic system in synaptic vesicles, synaptosomes and neural cells cultured from rat brain. Neurochem Int 81:41–47. https://doi.org/10.1016/j.neuint.2015.01.006
9. Nuñez-Figueredo Y, Ramírez-Sánchez J, Hansel G, Nicoloso E, Merino N, Valdes O, Delgado-Hernández R, Lagarto-Parra A et al (2014) A novel multi-target ligand (JM-20) protects mitochondrial integrity, inhibits brain excitatory amino acid release and reduces cerebral ischemia injury in vitro and in vivo. Neuropharmacology 85:517–527
10. Nuñez-Figueredo Y, Ramirez-Sanchez J, Delgado-Hernandez R, Porto-Verdecia M, Ochoa-Rodriguez E, Verdecia-Reyes Y, Marin-Prida J, Gonzalez-Durruthy M et al (2014) JM-20, a novel benzodiazepine-dihydropyridine hybrid molecule, protects mitochondria and prevents ischemic insult-mediated neural cell death in vitro. Eur J Pharmacol 726C:57–65
11. Núñez-Figueredo Y, Ramírez-Sanchez J, Hansel G, Pardo-Andreu GL, Merino N, Aparicio G, Delgado-Hernández R, García-Pupo L et al (2016) Therapeutic potential of the novel hybrid molecule JM-20 against focal cortical ischemia in rats. J Pharm Pharmacogn Res 4(4):153–158
12. Nunez-Figueredo Y, Pardo-Andreu GL, Ramirez-Sanchez J, Delgado-Hernandez R, Ochoa-Rodriguez E, Verdecia-Reyes Y, Naal Z, Muller AP et al (2014) Antioxidant effects of JM-20 on rat brain mitochondria and synaptosomes: mitoprotection against Ca(2)(+)-induced mitochondrial impairment. Brain Res Bull 109:68–76. https://doi.org/10.1016/j.brainresbull.2014.10.001
13. Longa EZ, Weinstein PR, Carlson S, Cummins R (1989) Reversible middle cerebral artery occlusion without craniectomy in rats. Stroke 20(1):84–91
14. Zhao H, Mayhan WG, Sun H (2008) A modified suture technique produces consistent cerebral infarction in rats. Brain Res 1246:158–166. https://doi.org/10.1016/j.brainres.2008.08.096
15. Lourbopoulos A, Karacostas D, Artemis N, Milonas I, Grigoriadis N (2008) Effectiveness of a new modified intraluminal suture for temporary middle cerebral artery occlusion in rats of various weight. J Neurosci Methods 173(2):225–234. https://doi.org/10.1016/j.jneumeth.2008.06.018
16. Schmid-Elsaesser R, Zausinger S, Hungerhuber E, Baethmann A, Reulen HJ (1998) A critical reevaluation of the intraluminal thread model of focal cerebral ischemia: evidence of inadvertent premature reperfusion and subarachnoid hemorrhage in rats by laser-Doppler flowmetry. Stroke 29(10):2162–2170
17. Cruz Portela LV, Oses JP, Silveira AL, Schmidt AP, Lara DR, Oliveira Battastini AM, Ramirez G, Vinade L et al (2002)

Guanine and adenine nucleotidase activities in rat cerebrospinal fluid. Brain Res 950(1–2):74–78
18. Pegg CC, He C, Stroink AR, Kattner KA, Wang CX (2010) Technique for collection of cerebrospinal fluid from the cisterna magna in rat. J Neurosci Methods 187(1):8–12. https://doi.org/10.1016/j.jneumeth.2009.12.002
19. Paxinos G, Watson C (2005) The rat brain in stereotaxic coordinates. Elsevier Academic Press
20. Peterson GL (1979) Review of the Folin phenol protein quantitation method of Lowry, Rosebrough, Farr and Randall. Anal Biochem 100(2):201–220
21. Lim CK (1986) HPLC of small molecules; a practical approach, vol 20 practical approach. IRL Press, Oxford
22. Schmidt AP, Tort AB, Silveira PP, Bohmer AE, Hansel G, Knorr L, Schallenberger C, Dalmaz C et al (2009) The NMDA antagonist MK-801 induces hyperalgesia and increases CSF excitatory amino acids in rats: reversal by guanosine. Pharmacol Biochem Behav 91(4):549–553. https://doi.org/10.1016/j.pbb.2008.09.009
23. Brouns R, De Vil B, Cras P, De Surgeloose D, Marien P, De Deyn PP (2010) Neurobiochemical markers of brain damage in cerebrospinal fluid of acute ischemic stroke patients. Clin Chem 56(3):451–458. https://doi.org/10.1373/clinchem.2009.134122
24. Burch JB, Augustine AD, Frieden LA, Hadley E, Howcroft TK, Johnson R, Khalsa PS, Kohanski RA et al (2014) Advances in geroscience: impact on healthspan and chronic disease. J Gerontol A Biol Sci Med Sci 69(Suppl 1):S1–S3. https://doi.org/10.1093/gerona/glu041
25. Unzeta M, Esteban G, Bolea I, Fogel WA, Ramsay RR, Youdim MB, Tipton KF, Marco-Contelles J (2016) Multi-target directed donepezil-like ligands for Alzheimer's disease. Front Neurosci 10:205. https://doi.org/10.3389/fnins.2016.00205
26. Dirnagl U, Simon RP, Hallenbeck JM (2003) Ischemic tolerance and endogenous neuroprotection. Trends Neurosci 26(5):248–254. https://doi.org/10.1016/s0166-2236(03)00071-7
27. Hutchinson PJ, O'Connell MT, Al-Rawi PG, Kett-White CR, Gupta AK, Maskell LB, Pickard JD, Kirkpatrick PJ (2002) Increases in GABA concentrations during cerebral ischaemia: a microdialysis study of extracellular amino acids. J Neurol Neurosurg Psychiatry 72(1):99–105
28. McCoy MK, Tansey MG (2008) TNF signaling inhibition in the CNS: implications for normal brain function and neurodegenerative disease. J Neuroinflammation 5:45. https://doi.org/10.1186/1742-2094-5-45
29. Whiteley W, Jackson C, Lewis S, Lowe G, Rumley A, Sandercock P, Wardlaw J, Dennis M et al (2009) Inflammatory markers and poor outcome after stroke: a prospective cohort study and systematic review of interleukin-6. PLoS Med 6(9):e1000145. https://doi.org/10.1371/journal.pmed.1000145
30. De la Calle JL, Paino CL (2002) A procedure for direct lumbar puncture in rats. Brain Res Bull 59(3):245–250
31. Sharma AK, Schultze AE, Cooper DM, Reams RY, Jordan WH, Snyder PW (2006) Development of a percutaneous cerebrospinal fluid collection technique in F-344 rats and evaluation of cell counts and total protein concentrations. Toxicol Pathol 34(4):393–395
32. Memezawa H, Minamisawa H, Smith ML, Siesjo BK (1992) Ischemic penumbra in a model of reversible middle cerebral artery occlusion in the rat. Exp Brain Res 89(1):67–78
33. Astrup J, Siesjo BK, Symon L (1981) Thresholds in cerebral ischemia—the ischemic penumbra. Stroke 12(6):723–725
34. Kirino T, Sano K (1984) Selective vulnerability in the gerbil hippocampus following transient ischemia. Acta Neuropathol 62(3):201–208
35. Petito CK, Morgello S, Felix JC, Lesser ML (1990) The two patterns of reactive astrocytosis in postischemic rat brain. J Cereb Blood Flow Metab 10(6):850–859. https://doi.org/10.1038/jcbfm.1990.141
36. Zhao H, Sapolsky RM, Steinberg GK (2006) Phosphoinositide-3-kinase/akt survival signal pathways are implicated in neuronal survival after stroke. Mol Neurobiol 34(3):249–270
37. Cai L, Stevenson J, Geng X, Peng C, Ji X, Xin R, Rastogi R, Sy C et al (2017) Combining Normobaric oxygen with ethanol or hypothermia prevents brain damage from thromboembolic stroke via PKC-Akt-NOX modulation. Mol Neurobiol 54(2):1263–1277. https://doi.org/10.1007/s12035-016-9695-7
38. Brazil DP, Yang ZZ, Hemmings BA (2004) Advances in protein kinase B signalling: AKTion on multiple fronts. Trends Biochem Sci 29(5):233–242. https://doi.org/10.1016/j.tibs.2004.03.006
39. Pekny M, Pekna M (2014) Astrocyte reactivity and reactive astrogliosis: costs and benefits. Physiol Rev 94(4):1077–1098. https://doi.org/10.1152/physrev.00041.2013
40. Anderson MA, Ao Y, Sofroniew MV (2014) Heterogeneity of reactive astrocytes. Neurosci Lett 565:23–29. https://doi.org/10.1016/j.neulet.2013.12.030
41. Escartin C, Bonvento G (2008) Targeted activation of astrocytes: a potential neuroprotective strategy. Mol Neurobiol 38(3):231–241. https://doi.org/10.1007/s12035-008-8043-y
42. Lee S, Park JY, Lee WH, Kim H, Park HC, Mori K, Suk K (2009) Lipocalin-2 is an autocrine mediator of reactive astrocytosis. J Neurosci 29(1):234–249. https://doi.org/10.1523/JNEUROSCI.5273-08.2009
43. Bi F, Huang C, Tong J, Qiu G, Huang B, Wu Q, Li F, Xu Z et al (2013) Reactive astrocytes secrete lcn2 to promote neuron death. Proc Natl Acad Sci U S A 110(10):4069–4074. https://doi.org/10.1073/pnas.1218497110
44. Stary CM, Sun X, Ouyang Y, Li L, Giffard RG (2016) miR-29a differentially regulates cell survival in astrocytes from cornu ammonis 1 and dentate gyrus by targeting VDAC1. Mitochondrion 30:248–254. https://doi.org/10.1016/j.mito.2016.08.013
45. Ouyang YB, Voloboueva LA, Xu LJ, Giffard RG (2007) Selective dysfunction of hippocampal CA1 astrocytes contributes to delayed neuronal damage after transient forebrain ischemia. J Neurosci 27(16):4253–4260